JOURNAL OF GUIDANCE, CONTROL, AND DYNAMICS
Vol. 29, No. 4, July–August 2006

# Flight Control Law Design for a Flexible Aircraft: Limits of Performance

Gilles Ferreres*
*ONERA, F-31055 Toulouse CEDEX, France*
and
Guilhem Puyou†
*AIRBUS France, 31060 Toulouse CEDEX 03, France*

**Limits of performance are explored when designing a flight control law for a flexible aircraft, especially the optimization of the wind comfort criterion under an actuator activity and roll-off constraint. When using a linear controller the order of which is free, the issue is either to check the feasibility of design specifications, or to compute the maximal achievable performance, or to study the tradeoff between the design specifications. To this aim the Convex Control Design Toolbox is developed, whose aim is the synthesis of multiple-input/multiple-output feedback and feedforward controllers with $H_\infty$ and $H_2$ specifications on a single plant model. Convex multimodel design is possible in the feedforward case, but parametric robustness specifications render the problem nonconvex in the feedback one.**

## I. Introduction

### A. Context

BECAUSE of the development of modern-day air transport requirements and the advances made in structural design, aircraft are becoming longer and more flexible. Thus, structural deformation and internal stress must be carefully monitored in order to both improve the passengers comfort and manage the loads levels. At the same time, it is still necessary to control the behavior of the flight mechanics: because of the closeness between the flight mechanics control bandwidth and the first structural modes, interactions between aerodynamics, flight control systems, and structural dynamics become more relevant.

Because of the complexity of the set of design specifications, these can no longer be met by single-objective optimized control laws. Multi-objective control laws must therefore be developed (see Ref. 1 for an overview and Ref. 2 for enhancements; see also Refs. 3 and 4 for applications to flexible aircraft and Refs. 5 and 6 for the multi-objective design of controllers with fixed order or structure, with aircraft applications). Among numerous approaches proposed in the literature, the convex closed-loop technique by Boyd and Barrat[7] appears especially attractive because $H_\infty$, $H_2$, and time-domain specifications are fully accounted for.

Moreover, this approach provides a solution to two related problems, the industrial interest of which is crucial. The first is to translate in a *direct* way a set of specifications into the design procedure, whereas the second is to check the feasibility of design specifications: does there exist a linear-time-invariant (LTI) controller, the order of which is free, that satisfies a set of specifications on an LTI closed loop? More generally, the issue is to compute the absolute limit of performance. This technique has two main applications in the aircraft design process. First, at the very beginning, when the structure is being defined, the computation of preliminary achievable control law performance rates is required in the optimization loop, especially to determine the critical load level and minimize the aircraft weight. Second, absolute limits of performance are also useful during the final control law tuning, to judge the quality of the implemented controller. For example, if a low-order controller can be synthesize which satisfies, for example, 90% of the maximal achievable performance, it can be considered quite satisfactory.

### B. Feedback and Feedforward Design

Consider the general architecture of a flight control law in Fig. 1. The issue is to design both feedback and feedforward controllers $K$ and $H$. Even if a two-degrees-of-freedom controller could be synthesized, the usual solution is first to synthesize the feedback controller, and then the feedforward one, noting moreover that their roles are quite distinct: $K$ is the only part that affects stability and disturbance rejection, while $H$ shapes the response to the pilot orders. Moreover, a static feedforward controller is usually used, which satisfies specifications on the closed-loop dc gain.

Nevertheless, many design specifications correspond to the response to pilot orders (template on the time-domain response to a fixed reference input signal, decoupling objective between pilot and structure), rather than to unmeasured disturbances (wind comfort criterion). If a static feedforward controller is used, the design of the feedback controller is made complex by the need to satisfy all design specifications, including those corresponding to the pilot orders. A better solution is to use dynamic feedforward controllers, especially when the set of specifications is complex and difficult to satisfy, noting that feedforward controllers can be synthesized using the same convex closed-loop design technique as for the feedback case. Concerning the feasibility of design specifications, in the absence of model uncertainty the achievable performance with the feedforward controller does not depend on the stabilizing feedback controller.[8] This is, however, no more true in the presence of uncertainty.

### C. Convex Closed-Loop Design

In the feedback case, the first step is to use Youla parameterization[9,10] to put the closed-loop transfer matrix under an affine form $T_1(s) + T_2(s)Q(s)T_3(s)$, where the $T_i(s)$ correspond to the interconnection of the open-loop plant with an initial fixed controller $K_0(s)$ while the design parameter is the stable transfer matrix $Q(s)$. Let $Q(s) = \sum_i \theta_i Q_i(s)$, where the filters $Q_i(s)$ are fixed while the $\theta_i$ are the design parameters. As a key property, the closed-loop transfer matrix $T_1(s) + T_2(s)Q(s)T_3(s)$ is affine with respect to the $\theta_i$, so that most nominal performance specifications and unstructured

Received 1 July 2005; revision received 12 August 2005; accepted for publication 16 August 2005. 

*Research Engineer, System Control and Flight Dynamics Department, DCSD, BP 4025; ferreres@onera.fr.

†Ph.D. Student, 316 route de Bayonne, ONERA-DCSD, BP 4025, F-3105 Toulouse Cedex, France, and SUPAERO, 10 Avenue Edouard Belin, 31055 Toulouse, France; currently Engineer, AIRBUS France.

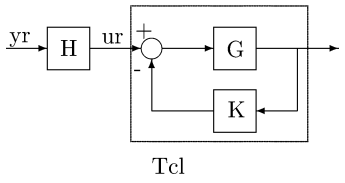


**Fig. 1 Feedback and feedforward controllers.**

robustness ones can be translated as convex constraints on the design parameters $\theta_i$, or as the minimization of a convex objective. The optimal value of the $\theta_i$, and thus of $Q(s)$, is computed with convex optimization; the optimal value of $K(s)$ is then deduced from $Q(s)$ and $K_0(s)$.

The principles of convex control design are exposed in the pionneering work of Boyd and Barrat.[7] Nevertheless many practical problems remained unsolved. Because of the industrial interest for the issue of checking the feasibility of design specifications, and thanks to a regain of interest for convex control design since the end of the 1990s, the subject is now more mature: see Ref. 11 for the development of some computational tools, Ref. 12 for an alternative method to check the feasibility of design specifications, and Ref. 13 for an aerospace application. Time-domain specifications are accounted for in Ref. 14, whereas convex control design is integrated in an overall design scheme in Ref. 15. In this context the Convex Control Design Toolbox[‡] was developed, which proposes a complete procedure for the design of feedback and feedforward controllers. Here is the procedure for the feedback case:

1) Design an initial controller, which is then put under the form of an observed-state feedback controller,[10,16,17] or direct design of an observed-state feedback controller. Note that any controller, whose order is at least equal to the order of the open-loop plant, can be put under the form of an observed-state feedback controller plus a nonzero value of the Youla parameter $Q(s)$ (if the controller order is strictly greater than the plant order).

2) Define a set of specifications: extended $H_\infty$ or $H_2$ specifications can be defined on finite frequency intervals, and analytic expressions of the templates are not necessary.

3) Choose an orthonormal basis of filters[18]: different poles can be introduced in the basis, corresponding to our physical knowledge of the plant, and the orthonormal nature of the basis largely reduces the potential numerical problems that can be encountered with the convex optimisation solver.

4) A specific effort was made on the computional burden when solving the convex optimization problem. A frequency-domain solution was developped in the spirit of Ref. 19. This is not an easy optimization problem because it has an infinite number of frequency-domain constraints and a large number of optimization parameters. [Because a large basis of $Q(s)$ is needed to check the feasibility of design specifications, it should even be theoretically infinite because the controller order is free.] The idea is to solve the optimization problem on a frequency gridding, and design specifications are then checked between the points of the gridding. If necessary, the gridding is refined, and a new convex optimization problem is solved. Moreover convex constraints at each point of the gridding are approximated as linear ones, using a cutting planes method.

5) Perform a balanced reduction of the optimal value of the Youla parameter $Q(s)$ under a performance constraint, noting that the order of the controller, which is typically equal to the sum of the orders of the open-loop plant and of $Q(s)$, can be (very) large. Reducing a controller under a performance constraint is a difficult problem, but a simple solution is proposed here in the specific context of convex closed-loop design. Nevertheless the order of the reduced controller is necessarily at least equal to the order of the open-loop plant model because just the Youla parameter $Q(s)$ is reduced.

6) Introduce structured robustness objectives with $DQ$ iterations, in the spirit of $DK$ iterations.[20] The issue is to ensure robust stability/performance of the closed loop in the presence of parametric uncertainties and neglected dynamics using the $\mu$ framework (see Refs. 20 and 21 and included references). The resulting optimization problem is biconvex with respect to $Q(s)$ and to the frequency-dependent scaling matrix $D$, corresponding to a $\mu$ upper bound.

Note finally that checking the feasibility of a set of design specifications with a constraint on the order or structure of the controller is still an open issue because a nonconvex optimization problem is obtained: if the design fails, it cannot be decided whether constraints are locally or globally infeasible.

The paper is organized as follows. Section II briefly presents the convex closed-loop design tools. Section III is devoted to the flexible aircraft application, whose numerical data are extracted from Ref. 21,[‡] noting that this sophisticated applicative example is used as the demo of the Toolbox. Concluding remarks end the paper.

## II. Convex Closed-Loop Design Tools

### A. Youla Parameterization

*1. Principle*

Consider the standard design problem of Fig. 2a, where

$$P = \begin{bmatrix} P_{11} & P_{12} \\ P_{21} & P_{22} \end{bmatrix}$$

is an augmented plant. The closed-loop transfer matrix $F_l(P, K) = P_{11} + P_{12}K(I - P_{22}K)^{-1}P_{21}$ is a highly nonlinear function of controller $K$, especially because of the need to invert $I - P_{22}K$. Suppose an initial stabilizing controller $K_0$, whose order is at least equal to the order of $P_{22}$, is available. Additional inputs and outputs $v$ and $e$ are introduced in $K_0$ (see Fig. 2b), with the key constraint that the transfer matrix between $v$ and $e$ is zero (see Fig. 2c). A solution to achieve this property is to put $K_0$ under the form of an observed state feedback controller[10] (see also the following). When connecting then a free stable transfer matrix $Q$ to these additional inputs and outputs, $F_l(P, K)$ can be rewritten as $T_1 + T_2QT_3$, where fixed transfer matrices $T_i$ depend on $P$ and $K_0$, while $Q$ is the design parameter.

The parameterization $T_1 + T_2QT_3$ covers the whole set of achievable closed loops: given any stabilizing feedback controller $K$, there exists a corresponding value of the stable Youla parameter $Q$ that gives the same closed loop [i.e., $F_l(P, K) = T_1 + T_2QT_3$] and conversely. As a consequence, let $Q = \sum_i \theta_i Q_i$, where filters $Q_i$ are fixed while the $\theta_i$ are the design parameters. If the infinite dimensional basis of filters $Q_i$ covers the whole set of asymptotically stable transfer matrices, the whole set of stabilizing feedback controllers $K$ is described. It thus becomes possible to check whether there exists a controller, whose order is free, that satisfies a set of design specifications.

*2. Case of an Observed State Feedback Controller*

Figure 3 presents the architecture of the controller, when using an observed state feedback controller (or a controller that was put under such form) as the initial one for Youla parameterization. Here $e$ is now the prediction error, while $v$ is an additive disturbance on the control input $u$. Assume that $x = \hat{x}$ at $t = 0$, and the open-loop plant model, which is embedded inside the observer, exactly coincides with the "true" open-loop plant. Despite a nonzero input $v$ the prediction error $e$ remains identically zero because the observer

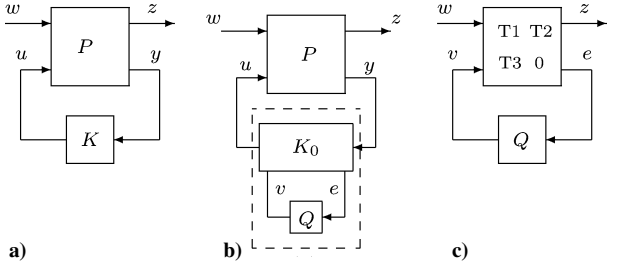


**Fig. 2 Closed loop structure: a) design problem and b,c) Youla parameterization.**

[‡]Data available online at http://www.cert.fr/dcsd/idco/perso/Ferreres/index.html [cited 2004].

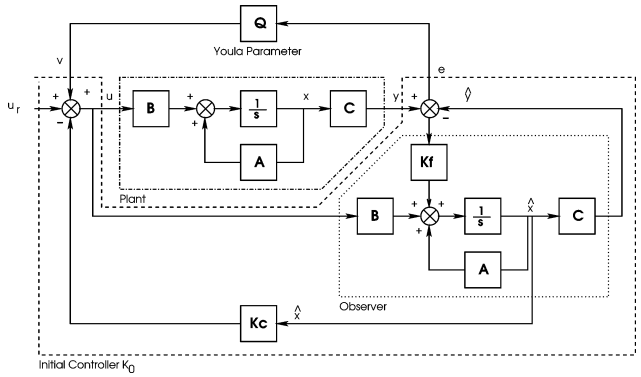


**Fig. 3 Youla parameterization with an observed state feedback controller.**

accounts for the measured disturbance $v$. Thus the transfer function between $v$ and $e$ is zero, as required. In the same way, the transfer function between $u_r = H(s)y_r$ and $e$ is zero, which means that a nonzero reference input $y_r$ just excites the closed-loop state feedback dynamics, not the observer one nor the dynamics of $Q(s)$, at least in the absence of model uncertainties.

*3. Choice of the Basis of Filters*

The orthonormal basis of Ref. 19 is used:

$$Q_i(s) = \frac{\sqrt{2Re(a_i)}}{s + a_i} \prod_{k=1}^{i-1} \frac{s - \bar{a}_k}{s + a_k}$$

The poles $-a_i$, which are chosen on the basis of our physical knowledge of the plant, are fixed. The special case of Laguerre filters is recovered by choosing the same pole for all $-a_i$, that is, $a_i = a\ \forall i$, but the basis of Ref. 18 is more interesting because different dynamics can be introduced in the same basis, so that if the choice of the poles $-a_i$ is adequate less filters are needed to cover the same part of the whole set of asymptotically stable transfer matrices. The computational burden is thus reduced.

### B. Convexity of Design Specifications

Generally speaking, a norm constraint on the closed-loop transfer matrix $T_1 + T_2QT_3$ is convex with respect to $Q = \sum_i \theta_i Q_i$. As a consequence, when constraining or minimizing the norm of various parts of the closed-loop transfer matrix $T_1 + T_2QT_3$, a convex optimization problem with convex constraints is obtained. Optimal values of the design parameters $\theta_i$ are computed; $Q(s)$ is then deduced as well as $K(s)$ (see Fig. 2b). Let $T(s, \theta) = T_1(s) + T_2(s)[\sum_i \theta_i Q_i(s)]T_3(s)$. Consider as an example a convex $H_\infty$ minimization objective, that is, the minimization of $\gamma$ under the constraint:

$$\bar{\sigma}[T(j\omega, \theta)] \leq \gamma\alpha(\omega) \forall \omega \in [\omega_1, \omega_2] \tag{1}$$

or the convex $H_\infty$ constraint $\bar{\sigma}[T(j\omega, \theta)] \leq \alpha(\omega)$, where $\alpha(\omega)$ is a fixed frequency-domain template. In the same spirit consider a convex constraint on the extended $H_2$ norm of the transfer matrix $T(s, \theta)$ on a finite frequency interval $[\omega_3, \omega_4]$:

$$\sqrt{\frac{1}{2\pi} \int_{\omega_3}^{\omega_4} Trace[T^*(j\omega, \theta)T(j\omega, \theta)]\, d\omega} \leq C \tag{2}$$

where $C$ is a constant, or the convex minimization of this extended $H_2$ norm, noting that the square of the $H_2$ norm in Eq. (2) can be approximated as a quadratic criterion $f_0 + f^T\theta + \theta^T Q\theta$ using a fine enough frequency gridding. Summarizing the following specifications can be accounted for in the Convex Control Design Toolbox: $H_\infty$ minimization or constraint, $H_2$ minimization or constraint, $\mu$ minimization or constraint (see Sec. II.E). Time-domain specifications could also be introduced because they correspond to additional linear-programming (LP) constraints.[14]

Consider again Fig. 1, and assume that $K(s)$ is fixed. The feedforward controller $H(s) = \sum_i \theta_i H_i(s)$ is to be synthesized, which simultaneously satisfies design specifications on several closed-loop models. Let $G(s) = G_i(s)$, so that the closed-loop transfer matrix without feedforward becomes $T_{cl,i}(s)$. The idea is simply to stack into a single convex optimization problem all $H_\infty/H_2$ constraints and minimization objectives for all closed-loop models $T_{cl,i}(s)H(s)$. Moreover the design specifications will be satisfied on the polytope of closed-loop systems, that is, if $T_{cl,1}(s)H(s)$ and $T_{cl,2}(s)H(s)$ satisfy the design specifications, $[\lambda T_{cl,1}(s) + (1 - \lambda)T_{cl,2}(s)]H(s)$ satisfies the design specifications $\forall\lambda \in [0, 1]$.

As a final point, unlike the feedforward case the convex multimodel design of a feedback controller appears impossible for two reasons. First, the open-loop plant model, which is embedded inside the observer, must exactly coincide with the "true" one to obtain the affine form $T_1 + T_2QT_3$. Second, a convex multimodel design of $Q$ is possible, but when deducing $K$ from $Q$ and from the initial observed state feedback controller (see Fig. 3) $K$ will depend on the embedded open-loop plant model, that is, a single feedback controller $K$ cannot be obtained for all plant models.

### C. Principle of the Cutting Planes Method

We just explained the principle of this classical method (see Ref. 7 for details). The idea is to approximate the nondifferentiable convex constraint (1) at $\theta = \theta^0$ by an affine one:

$$\bar{\sigma}[T(j\omega, \theta^0)] + S^T(\theta - \theta^0) \leq \gamma\alpha(\omega) \tag{3}$$

where $S$ is called a subgradient. Indeed, for all $\theta$

$$\bar{\sigma}[T(j\omega, \theta^0)] + S^T(\theta - \theta^0) \leq \bar{\sigma}[T(j\omega, \theta)]$$

When approximating Eq. (1) at differents points $\theta = \theta^i$ and at different frequencies $\omega = \omega_i$, all of these affine constraints (3) can be stacked into an LP constraint

$$A\begin{bmatrix}\theta \\ \gamma\end{bmatrix} \leq b$$

Generally speaking, when considering the minimization of a convex objective under convex constraints a lower bound of the minimal value $\gamma^*$ of the objective is computed as the minimal value of $\gamma$ under the preceding LP constraints. The idea is then to refine this affine approximation of the convex optimization problem until $\gamma^*$ is computed with a satisfactory accuracy, as illustrated by the following sketch of algorithm:

1) Compute the value $\tilde{\theta}$ of $\theta$ that minimizes $\gamma$ under the LP constraints. Let $\gamma_{lb}$ the associated minimal value of $\gamma$.

2) Compute an upper bound $\gamma_{ub}$ of $\gamma^*$, noting that any value of $\theta$ satisfying the constraints provides an upper bound. If the gap between the bounds is close enough stop. Otherwise approximate convex constraints and minimization objectives at $\theta = \tilde{\theta}$ and at critical frequencies, where constraints are the most violated. Return to step 1.

The use of a cutting planes method renders possible a progressive convex control design in the case of a large number of optimization parameters $\theta_i$. If there are, for example, 80 optimization parameters, only the first eight optimization parameters are first used, and the associated value of the minimized objective is computed. Then the first 16 optimization parameters are used, and the value of the minimized objective is here again computed until all 80 optimization parameters are used. The decrease of the minimized objective is visualized as a function of the number of optimization parameters (see the example of Fig. 4). If the value of the minimized objective tends towards an asymptotic value, this means that adding more filters is useless, that is, the value of the minimized objective, corresponding to an infinite dimensional basis of filters, is obtained.

During this progressive design, subgradients are kept from an optimisation to an other in order to save a large amount of computational time. In the same way, it is possible to study the tradeoffs between the design specifications. The issue is to minimize an objective under several constraints, where one of these constraints takes several values. Depending on the hardness of this constraint, it is more

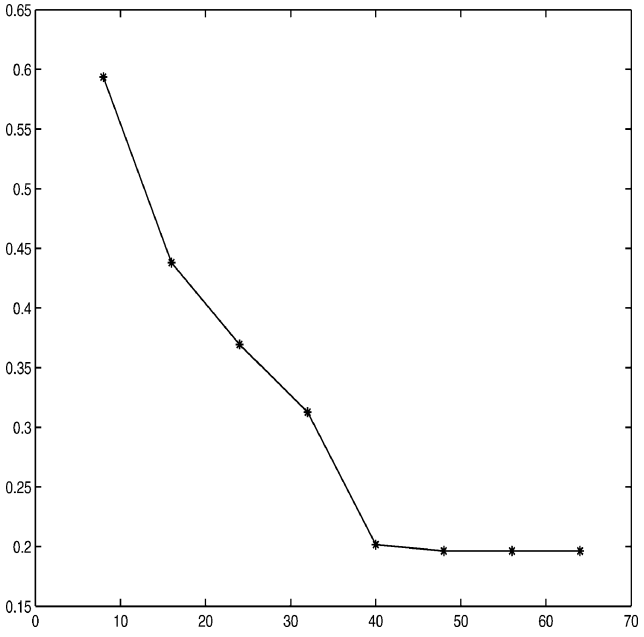


**Fig. 4 Minimized value of the wind comfort criterion $\alpha$ as a function of the number of used filters $Q_i(s)$.**

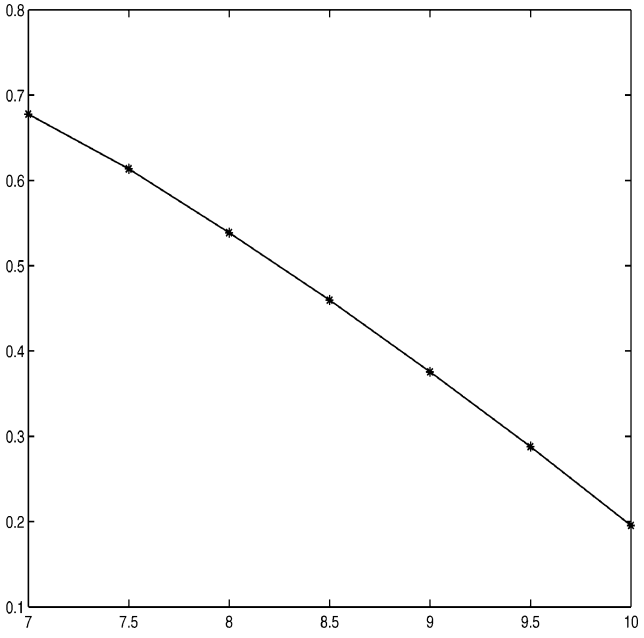


**Fig. 5 Minimized value of the wind comfort criterion $\alpha$ as a function of the cutoff frequency $\omega_0$ (in rad/s).**

or less possible to minimize the objective: see the example of Fig. 5, where the $x$ axis represents a cutoff frequency while the $y$ axis represents the minimized objective. The lower the cutoff frequency is, the harder the constraint is, and thus the higher the minimized objective is. Here again it is possible to save a large amount of computational time by keeping subgradients from an optimization to an other.

### D. Reduction of the Youla Parameter

A large basis of filters is necessary to check the feasibility of design specifications, so that the order of $Q(s)$ is (very) high. We would like to reduce it under a performance preservation constraint. Let $Q_r(s)$ be the reduced Youla parameter. The issue is to minimize the reduction error between the closed-loop transfer matrices:

$$T_1(s) + T_2(s)Q(s)T_3(s) - T_1(s) - T_2(s)Q_r(s)T_3(s)$$
$$= T_2(s)[Q(s) - Q_r(s)]T_3(s)$$

The classical balanced reduction method is used to reduce $Q(s)$ with weighting functions $T_2(s)$ and $T_3(s)$. Note that the poles of the reduced Youla parameter $Q_r(s)$ do not belong to the initial set of poles of $Q(s)$ and that the stability of $Q_r(s)$ is not guaranteed. In the case of a feedforward controller $H(s)$ (see Fig. 1), the issue is to minimize the reduction error $T_{\mathrm{cl}}(s)[H(s) - H_r(s)]$, so that the balanced reduction method can be used with weighting function $T_{\mathrm{cl}}(s)$.

### E. *DQ* Iterations

Let $M(s) - \Delta$ be a standard interconnection structure (see Refs. 20 and 21 and included references), where $\Delta$ is a structured model perturbation and $M$ is the closed-loop transfer matrix $T_1 + T_2 \sum_i \theta_i Q_i T_3$. With reference to the complex $\mu$ upper bound, let the scaling matrix $D$ satisfying for all $\Delta D \Delta = \Delta D$. The issue is to find design parameters $\theta_i$ and frequency-dependent scaling matrices $D(\omega)$ minimizing $\gamma$ under the constraints:

$$\bar{\sigma}\left\{D(\omega_k)\left[T_1(j\omega_k) + \sum_i \theta_i T_2(j\omega_k)Q_i(j\omega_k)T_3(j\omega_k)\right]D^{-1}(\omega_k)\right\}$$
$$\leq \gamma$$

where $\gamma$ is a $\mu$ upper bound, and a guaranteed value of the robustness margin is obtained as $1/\gamma$. For a given design frequency gridding $(\omega_k)_{k\in[1,N]}$, one optimizes with respect to the $\theta_i$ (using the same cutting planes method as above), then with respect to scalings $D(\omega)$, then with respect to the $\theta_i$ .... Nominal $H_2$ and $H_\infty$ performance constraints can be added in this nonconvex minimization problem.

Once the optimization is performed, $H_\infty$ specifications are checked between the points of the design frequency gridding, namely, on an a priori fixed fine validation gridding. If they are not satisfied, a worst-case frequency, corresponding to the maximal violation of the constraints, is added to the design gridding. In the same way the robustness objective is checked but without frequency gridding, that is, with a frequency sweeping technique that is computationally (very) efficient.[22]

*Remarks:*

1) When designing the controller, all uncertainties are assumed to be complex. But when a posteriori computing the robustness margin, the real nature of parametric uncertainties can be accounted for using the mixed $\mu$ upper bound with additional scaling matrix $G$.

2) Unlike in many $\mu$-synthesis schemes, no analytic expression is needed for $D(\omega)$; their value is just needed on the design frequency gridding.

## III. Application

### A. Model and Design Specifications

*1. Model Description*

The issue is to design a lateral flight control system, whose structure is given on Figs. 1 and 3 for a flexible transport aicraft. The model, whose order is 21 with two inputs (aileron and rudder deflections) and four outputs $ny$, $p, r, \phi$, contains four rigid states (the sideslip angle $\beta$, the rotational rates $p$ and $r$, and the bank angle $\phi$), 12 flexible states corresponding to six bending modes, and five actuators states.[21] This state-space model is built by coupling rigid and elastic body models (see Fig. 6). The evaluation methods are described in Ref. 23 and summarized in Ref. 24. The two models are coupled by connecting measurement outputs at the same structural point of the aircraft. Other methods for translating interactions between rigid and flexible bodies are known, but they are more complex, and the one given here provides a good enough representation.

The design specifications set we use next is a simplified version of the one in Ref. 15, which contains five main types of criteria: robustness, handling qualities, comfort, loads, and actuators. Our simplified version does not tackle the load control problem, and the comfort level enhancement is achieved by minimizing the $H_\infty$ norm on an acceleration output, whereas the original criterion is a mixed $H_2/H_\infty$ one on a more sophisticated transfer function, containing a wind spectrum and weighting functions that characterize the passengers' feeling.

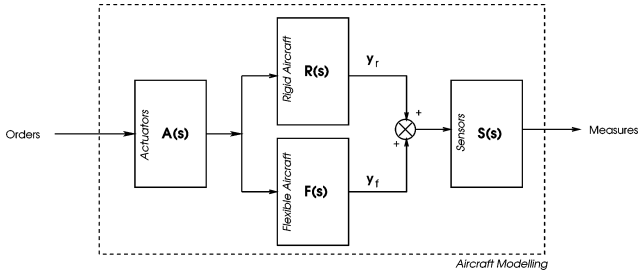


**Fig. 6 Aircraft modeling.**

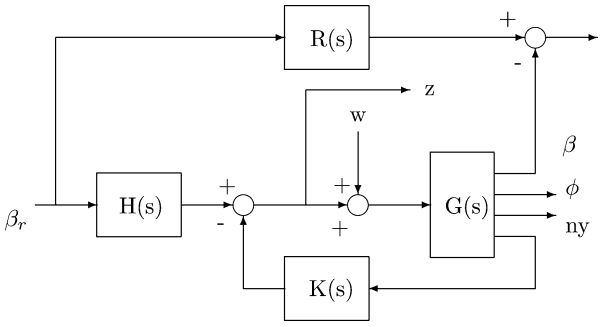


**Fig. 7 Feedback and feedforward design scheme.**

*2. Design Specifications: The Feedback Part*

Figure 7 presents the feedback and feedforward design scheme. Let $M_1(s)$ [respectively, $M_2(s)$] be the closed-loop single-input/single-output (SISO) transfer function between the perturbation $w_1$ (respectively, $w_2$) on the first (respectively second) aircraft input and the acceleration $ny$, and $M_3(s)$ be the closed-loop multiple-input/multiple-output transfer matrix between perturbation $w$ and $z$. Let also $M_{1,\mathrm{OL}}(s)$ [respectively, $M_{2,\mathrm{OL}}(s)$] be the open-loop SISO transfer function between the first (respectively second) aircraft input and $ny$. The feedback design problem is as follows:

1) Spec # 1. Wind comfort on the nominal closed loop: Let $\mathcal{M}_{1,\mathrm{OL}}$ (respectively $\mathcal{M}_{2,\mathrm{OL}}$) be the peak value of $|M_{1,\mathrm{OL}}(j\omega)|$ (respectively $|M_{2,\mathrm{OL}}(j\omega)|$) between 5 and 25 rad/s. Inside this frequency interval the issue is to minimize $\alpha$ under the constraint:

$$|M_1(j\omega)| \le \alpha\mathcal{M}_{1,\mathrm{OL}}, \qquad |M_2(j\omega)| \le \alpha\mathcal{M}_{2,\mathrm{OL}}$$

where $\alpha = 1$ corresponds to the open loop, that is, to $K(s) = 0$.

2) Spec # 2. Actuator activity and roll-off constraint on the nominal closed loop: Let the template be

$$F(s) = G\Big/\Big\{\Big[1 + 1.4(s/\omega_0) + s^2\Big/\omega_0^2\Big](1 + s/\omega_0)\Big\}$$

At all frequencies the constraint is

$$\bar{\sigma}[M_3(j\omega)] \le |F(j\omega)|$$

The issue is to constrain the actuators' activity at low and middle frequencies while ensuring a satisfactory roll-off, especially because of high-frequency unmodeled bending modes (represented as additive neglected dynamics on the plant model, so that a stability margin could be deduced). Here $\omega_0$ and $G$ are tuning parameters; a typical value is $\omega_0 = 10$ rad/s and $G = 10$ dB.

3) Spec # 3. Parametric robustness: Closed-loop stability must be ensured despite $\pm 4\%$ of simultaneous uncertainties in the frequencies of the six bending modes.

*Remark*: The additive disturbance input $w$ is a simple way to represent a wind input. The wind comfort criterion can then be easily tested in flight, by adding a disturbance input on the control input, and the open and closed loops are easily compared because $\alpha < 1$ means that the closed-loop criterion is reduced with respect to the open-loop one. Nevertheless a "true" wind input could also be used, if available with the model, to define a more sophisticated comfort criterion.[15]

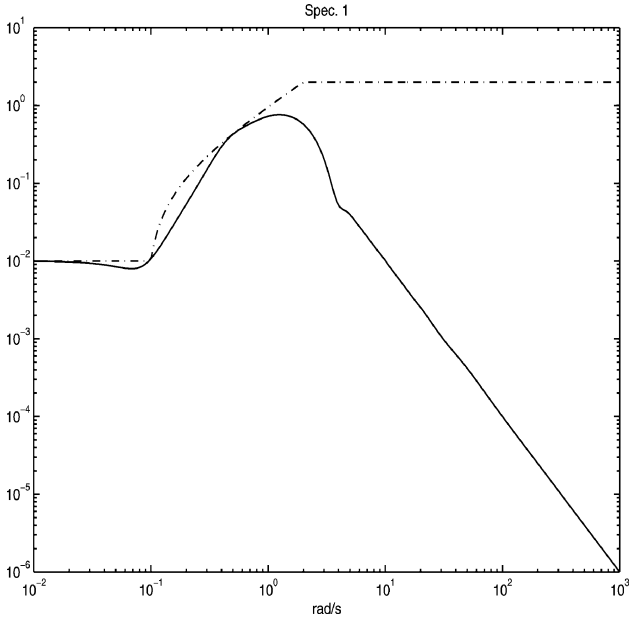


**Fig. 8 Design specification # 1 on the optimized feedforward controller (32 filters).**

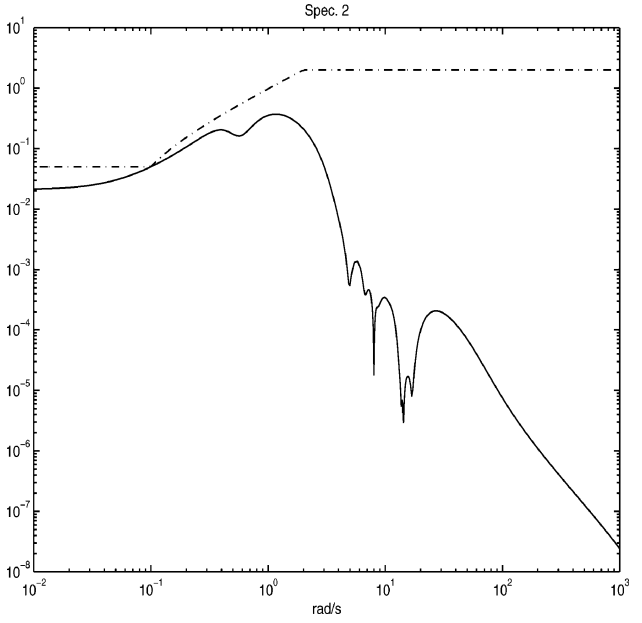


**Fig. 9 Design specification # 2 on the optimized feedforward controller (32 filters).**

*3. Design Specifications: The Feedforward Part*

The issue is to shape the response to a reference sideslip angle $\beta_r$. The design specifications are as follows:

1) Spec # 1. Rigid performance on the nominal closed loop: The error between the reference model $R(s) = 1/(s^2 + 1.4s + 1)$ and the nominal closed-loop transfer function between $\beta_r$ and $\beta$ must remain below a template (see Fig. 8). (The dashed plot corresponds to the template, which is defined by four frequency points: 0, 0.1, 2, and 1000 rad/s. A linear interpolation is used between these points, but the interpolation does not seem linear because of the logarithmic plot.)

2) Spec # 2. Decoupling on the nominal closed loop: The nominal closed-loop transfer function between $\beta_r$ and $\phi$ must remain below a template (see Fig. 9).

3) Spec # 3. Aircraft-pilot decoupling despite parametric uncertainties: On the output $ny$ the peaks that are caused by flexible modes are to be minimized on all 65 models, that is, the nominal

one and the $2^6 = 64$ aircraft models, which are generated when considering extremal uncertainties of $\pm 4\%$ in the frequencies of the six-bending modes.

### B. Design of an Initial $H_\infty$ Controller

Classical $H_\infty$ control shapes closed-loop transfer matrices, whereas loop-shaping $H_\infty$ control shapes the open loop. Let $G(s)$ be the plant model. Pre- and postcompensators $W_1(s)$ and $W_2(s)$ are determined, so that the ideal open loop is $G_s(s) = W_2(s)G(s)W_1(s)$. The issue is to preserve this open-loop shape as much as possible. To this aim, loop-shaping $H_\infty$ control synthesizes a controller $K_\infty(s)$, which stabilizes $G_s$ while maximizing the robustness to neglected dynamics on the coprime factors of $G_s$. A direct solution to this specific $H_\infty$ problem, without $\gamma$ iterations, is available, as well as a natural observed-state feedback form for $K_\infty(s)$ (Refs. 16 and 17). The final controller is $W_1(s)K_\infty(s)W_2(s)$.

A static output feedback $K_{\text{ref}}$ is classically synthesized for the rigid plus actuators aircraft model, which places the main closed-loop poles. The time-domain performance is satisfactory [see the dashed lines of Fig. 10 (which corresponds to step responses on the reference inputs $\beta_r$ and $\phi_r$ with a static feedforward controller]. But the interconnection of $K_{\text{ref}}$ with the complete rigid plus flexible plus actuators model is unstable. Let the augmented plant $G_s(s) = K_{\text{ref}}G(s)$. Loop-shaping $H_\infty$ control synthesizes $K_\infty(s)$, and the final controller is $K(s) = K_\infty(s)K_{\text{ref}}$. On Fig. 10 the time-domain performance of the complete rigid plus flexible plus actuators model (solid line) looks like the one in dashed line. Moreover the wind comfort criterion is satisfactory [see Figs. 11 and 12, where the dashed (respectively solid) plot corresponds to the open (respectively closed) loop transfer function $M_{i,\text{OL}}(s)$ (respectively $M_i(s)$)], and the roll-off specification is also satisfied. The performance of this initial controller, whose design is very simple, is thus quite satisfactory.

*Remarks:*

1) Because $K_{\text{ref}}$ is static and the order of $K_\infty(s)$ is equal to the one of $G(s)$, the order of $K(s)$ is 21, like the open-loop plant model.

2) With respect to Fig. 3 and Sec. II.A.2, the feedback controllers, which will be obtained in the next sections by adding nonzero values of $Q(s)$, will have the same time-domain response to the reference input $\beta_r$, at least for the nominal closed loop.

### C. Convex Design of a Feedback Controller and Computation of Design Tradeoffs

The basis of Ref. 18 is used with the following poles, whose damping ratio is 0.7:

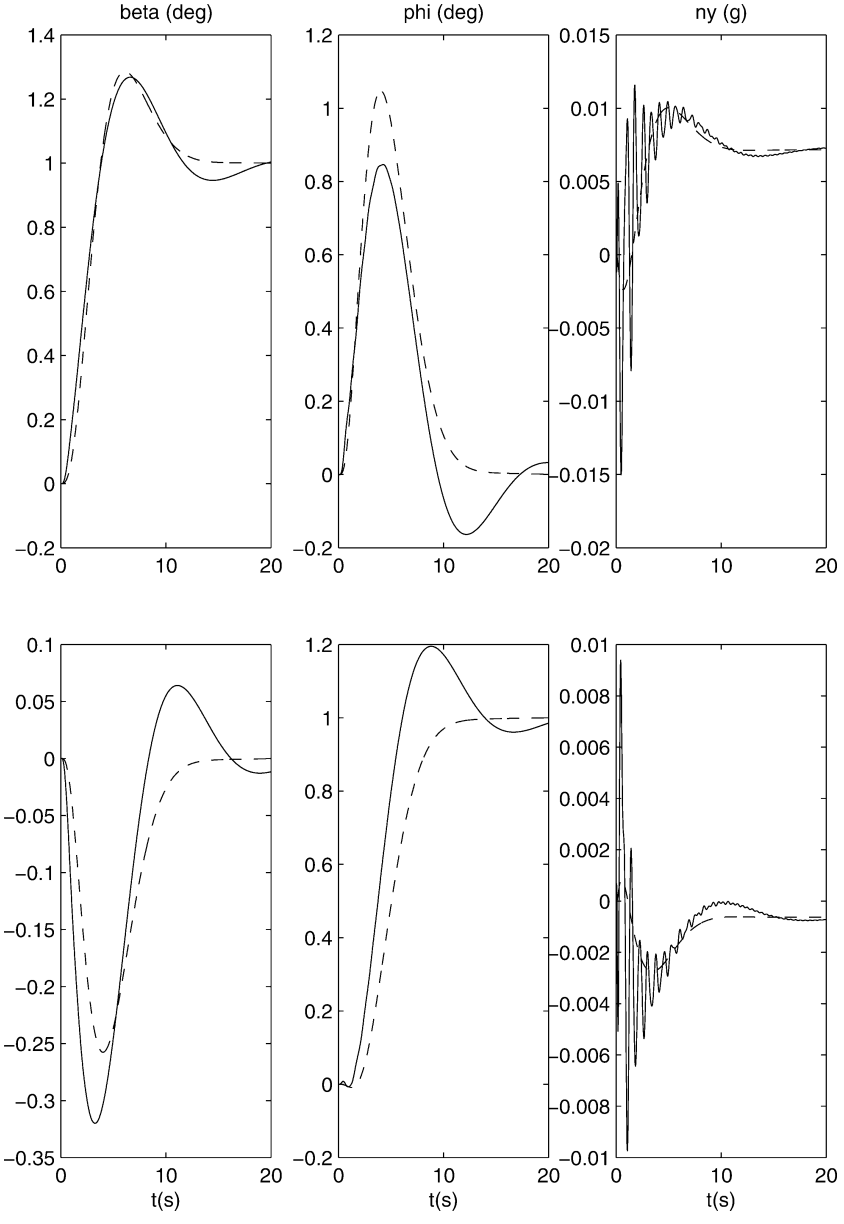


**Fig. 10 Step responses to a reference input $\beta_r$ or $\phi_r$ on the rigid and complete aircraft models.**

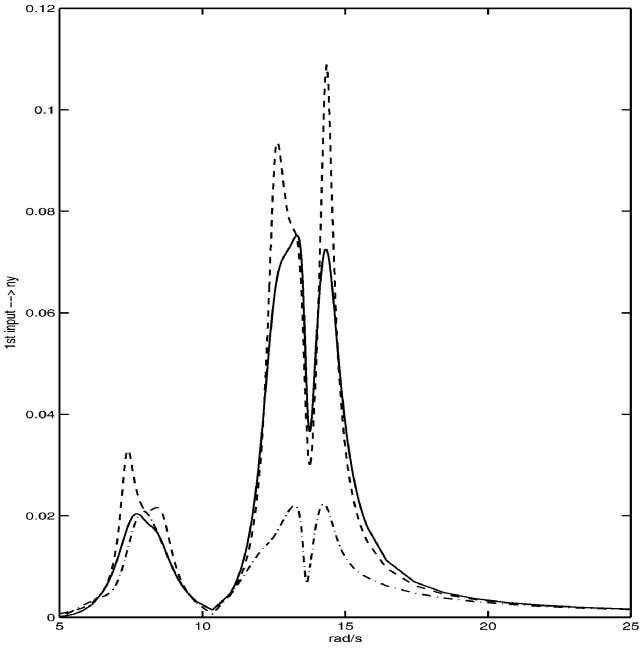


**Fig. 11 Wind comfort criterion for the first input, that is, $|M_1(j\omega)|$ as a function of $\omega$.**

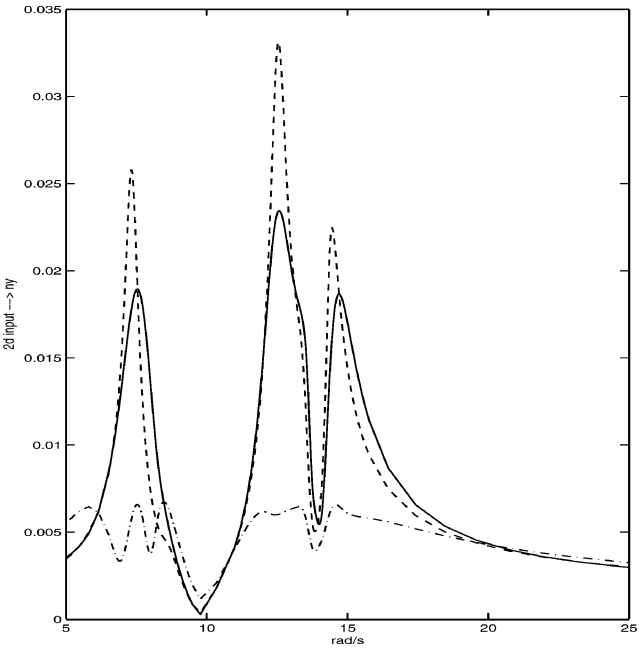


**Fig. 12 Wind comfort criterion for the second input, that is, $|M_2(j\omega)|$ as a function of $\omega$.**

$$5\frac{-1\pm j}{\sqrt{2}}\ 8\frac{-1\pm j}{\sqrt{2}}\ 12\frac{-1\pm j}{\sqrt{2}}\ 15\frac{-1\pm j}{\sqrt{2}} \tag{4}$$

Because $Q(s)$ has two outputs and four inputs, this corresponds to 64 filters. The frequencies of these poles are chosen inside [5 rad/s, 25 rad/s], where the wind comfort criterion is defined. (This corresponds to the range of frequencies of open-loop bending modes.) The set of design specifications is the one of Sec. III.A.2, that is, the minimization of 2 $H_\infty$ objectives under an $H_\infty$ constraint. (The parametric robustness specification will be accounted for in the next section.) A progressive design is performed with 8, 16, ..., 64 filters (see Sec. II.C). An asymptotic value for the minimized comfort criterion $\alpha \approx 0.2$ is obtained on Fig. 4, which suggests that the value $\alpha$ of the minimized objective, corresponding to an infinite dimensional basis of filters, is obtained. The computational time is 689 s (11 min) on a SUN Sparc station, which is quite reasonable when considering the complexity of this high dimensional problem. See also the dash-dot plot on Figs. 11 and 12, which represents the closed-loop response with the optimal controller.

*Remarks:*

1) Our computational experience is that the computational cost of a progressive design remains close to the one of a one-shot design, and more information is produced.

2) The same design is performed with an other initial controller, namely, a true observed state feedback controller whose design is rough, so that its performance is less satisfactory. Eighty filters must now be used, and the computational time is higher, but the asymptotic value of $\alpha$ remains the same, which is logical because this asymptotic value does not depend on the initial controller. But the better performing this one is, the simpler the design of $Q(s)$ is to obtain the asymptotic achievable performance.

3) It would also be possible to introduce $H_2$ constraints or minimization objectives on $M_1(s)$ and $M_2(s)$.

4) In the context of our example, the choice of the poles of the basis does not appear especially sensitive; several well-damped poles were just chosen between 5 and 25 rad/s, and it was especially unecessary to retune this choice to obtain better results because the asymptotic value of the minimized objective, corresponding to an infinite dimensional basis of filters, is already obtained. But in other situations this choice can appear more critical; it might especially appear necessary to choose less well-damped poles to improve the results and/or obtain the asymptotic value. The minimal number of filters that are necessary to compute the asymptotic value of the minimized objective obviously depends on the choice of the basis: a bad choice means that more filters are needed.

The order of the optimal $Q(s)$ is 12, which is already low. [Twelve corresponds to the minimal realization of $Q(s)$, computed with the MATLAB® routine minreal.m. It seems difficult to guess the order of the optimal $Q(s)$, even if the number of filters is a priori known because the order of the minimal realization can be (much) lower than the initial one.] When $Q(s)$ is directly reduced without weighting function, eliminating a single state already increases the wind comfort criterion, which becomes 0.238 on the first input and 0.312 on the second one (instead of 0.206 for the optimal controller). The roll-off constraint is also violated. When eliminating two states, the wind comfort criterion becomes 0.628 on the first input and 1.045 on the second one.

When weighting functions are used, the result is much better. Remember that the issue is to minimize the reduction error $T_2(s)[Q(s) - Q_r(s)]T_3(s)$. First all possible inputs and outputs of $T_1(s) + T_2(s)Q(s)T_3(s)$ are used, that is, the two additive perturbations $w$ on the aircraft inputs, the acceleration output $ny$ and the two controller outputs $z$ (see Fig. 7). When eliminating two states, the wind comfort criterion becomes 0.202 on the first input and 0.279 on the second one. The roll-off constraint is slightly violated. When only considering the two additive perturbations $w$ on the aircraft inputs and the acceleration output $ny$, the wind comfort criterion is perfectly preserved, that is, 0.206 on the first input and 0.207 on the second one (instead of 0.206 for the optimal controller). Here again the roll-off constraint is slightly violated. The weighting functions $T_2(s)$ and $T_3(s)$ are thus crucial to preserve closed-loop performance.

It seems impossible to remove more states in $Q(s)$ while preserving the wind comfort criterion, but 10 states in the Youla parameter seem not too much to reduce the wind confort criterion from $\alpha \approx 0.7$ with the initial $H_\infty$ controller to $\alpha \approx 0.2$ with the optimal one (see Figs. 11 and 12). Nevertheless it would be interesting to reduce then the feedback controller $K(s)$, whose order is still $31 = 21$ (the order of the open loop plant) $+10$ (the order of the reduced Youla parameter), under a closed-loop modal performance preservation constraint, as proposed in Ref. 15.

We finally study the tradeoff between the cutoff frequency $\omega_0$ and the minimized value $\alpha$ of the comfort criterion. The same basis (4) of $Q(s)$ is used, as well as the same initial $H_\infty$ controller. Here $\omega_0$ belongs to the set 7, 7.5, 8, ..., 10 rad/s. (The roll-off specification seems infeasible below 7 rad/s.) The result is presented on Fig. 5.

The computational time for the whole curve is 1649 s (27 min), while the computational time for the single value $\omega_0 = 10$ rad/s was 689 s, that is, 42% of 1649 s. This illustrates the fact that it is possible to save a large amount of computational time by keeping subgradients from an optimization to an other.

### D. Nonconvex Design of a Robust Feedback Controller

The issue is to ensure robust stability in the face of parametric uncertainties on the frequencies of the bending modes. The linear-fractional-transformation model is extracted from Ref. 21. The issue is to maximize the robustness margin under the roll-off constraint of Sec. III.A.2 and under a constraint on the wind comfort criterion $\alpha \leq 0.75$. This threshold is chosen so that the initial controller satisfies the constraints, that is, the issue is to observe the increase of the robustness margin between the initial and final controllers.

More precisely we would like to illustrate that a few filters are enough to significantly increase the margin, so that we choose a basis of 24 filters with poles $-5$, $-10$, and $-15$. The computational time is only 184 s (3 min). The robustness margin of the initial controller is $\pm 1.65\%$ if parametric uncertainties are assumed to be complex and $\pm 3.47\%$ if their real nature is accounted for. Thus the closed loop remains stable despite simultaneous variations of $\pm 3.47\%$ on all six frequencies of the bending modes.

The robustness margin of the optimized controller is $\pm 2.56\%$ if parametric uncertainties are assumed to be complex and $\pm 4.33\%$ if their real nature is accounted for. By optimizing with only a few filters, the parametric robustness properties were significantly improved while keeping the good nominal performance properties of the initial controller.

### E. Convex Design of a Robust Feedforward Controller

The feedback controller obtained at the end of the preceding section is now fixed. The issue is to synthesize a robust feedforward controller $u_r = H(s)\beta_r$ that satisfies the set of design requirements of Sec. III.A.3. The following poles are chosen for the basis of 32 filters:

$$\frac{-1 \pm j}{\sqrt{2}}\ 3\frac{-1 \pm j}{\sqrt{2}}\ 5\frac{-1 \pm j}{\sqrt{2}}\ 7\frac{-1 \pm j}{\sqrt{2}}\ 9\frac{-1 \pm j}{\sqrt{2}}\ 11\frac{-1 \pm j}{\sqrt{2}}$$

$$13\frac{-1 \pm j}{\sqrt{2}}\ 15\frac{-1 \pm j}{\sqrt{2}}$$

Let $\alpha^*$ be the minimized value of the peaks that are caused by flexible modes on all 65 models. Then $\alpha^*$ is computed for the first eight filters, then for the first 16 and 24 filters, and finally for all of the 32 ones. Figure 13 presents $\alpha^*$ as a function of the number of filters. Here $\alpha^* = 3.157e{-}04$ for 32 filters, and the computational time is only 1126 s (19 min) despite the large number of flexible models. Figures 8, 9, and 14 present the performance of the final controller. We have illustrated through this example that it is possible to use a large set of flexible models and frequency responses while keeping a reasonable computational requirement and without an explosion of the required memory. (A large amount of frequency responses is to be stored on the design frequency gridding, but this frequency gridding is refined to minimize its size, and the number of design models is also minimized.)

The order of the optimal feedforward controller is 16. We focus on the performance of the nominal closed-loop model, that is, the closed-loop model used as the weighting function for reduction is the nominal one $T_{\mathrm{cl},1}(s)$. $T_{\mathrm{cl},1}(s)$ has two inputs $u_r$ and three outputs that are used by the design specifications: $ny$, $\phi$, and the error between the reference model and the output $\beta$ of the closed loop. Let $T(s)$ be the part of $T_{\mathrm{cl},1}(s)$ corresponding to the transfer function between $u_r$ and $ny$. The balanced reduction method is applied to $T(s)H(s)$ to focus on the preservation of the performance on $ny$.

The first row of Table 1 presents the value of the peak corresponding to design specification 3 on the nominal closed-loop model, when reducing $H(s)$ to order 15, 14, ... and 8, noting that design specifications 1 and 2 are still satisfied. (Values inside the table can be less than the optimal one because the peak value of the criterion is not necessarily obtained on the nominal closed-loop model.) The reduced feedforward controller of order 11 is quite satisfactory. Note nevertheless that the performance of the other closed-loop models is much less satisfactory (up to $1.347e{-}03$ instead of the optimal value $3.157e{-}04$ !).

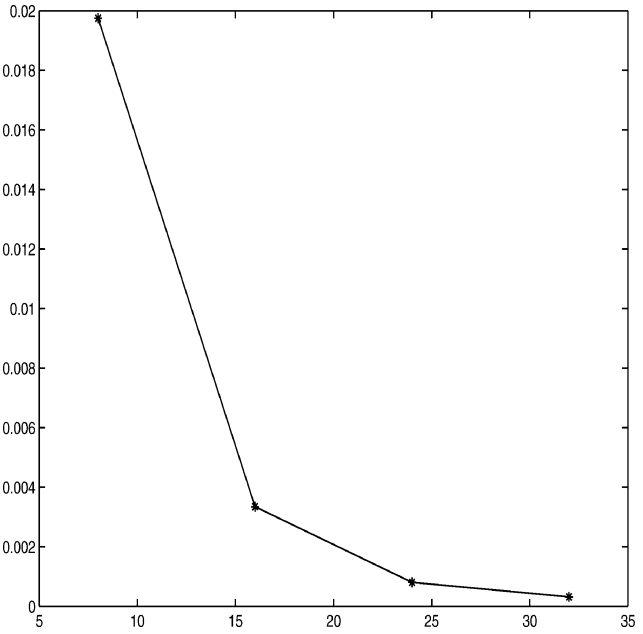


**Fig. 13 Decrease of the minimized value of the peaks, which are caused by flexible modes on all 65 models, as a function of the number of filters.**

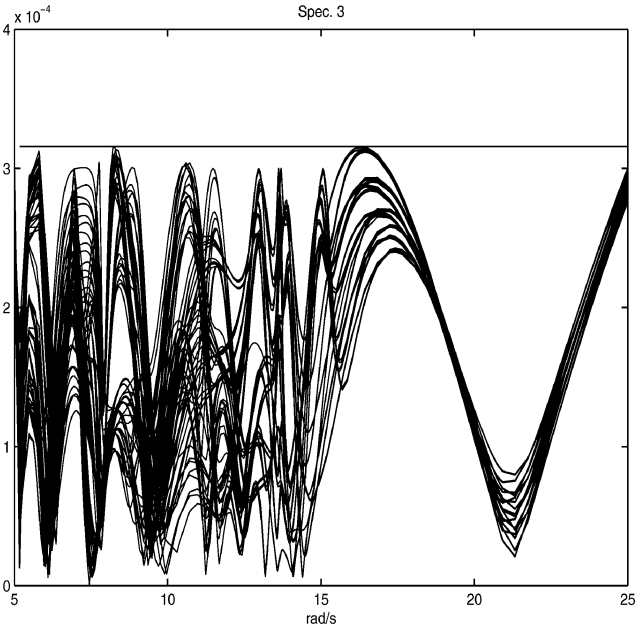


**Fig. 14 Design specification # 3 on the optimized feedforward controller (32 filters).**

**Table 1 Value of the peak on the nominal closed loop**

| Reduction order | 16 | 15 | 14 | 13 | 12 | 11 | 10 | 9 | 8 |
|---|---|---|---|---|---|---|---|---|---|
| With $T(s)$ weighting function | $2.878e{-}04$ | $3.373e{-}04$ | $3.137e{-}04$ | $2.889e{-}04$ | $3.911e{-}04$ | $3.098e{-}04$ | $3.682e{-}04$ | $4.614e{-}04$ | $7.156e{-}04$ |
| Without weighting function | $2.878e{-}04$ | $5.085e{-}04$ | $4.611e{-}04$ | $6.969e{-}04$ | $6.263e{-}04$ | $1.699e{-}03$ | $1.430e{-}03$ | $4.685e{-}03$ | $4.939e{-}03$ |

The second row of Table 1 presents the same result when directly reducing $H(s)$ without weighting function. At order 11, the peak corresponding to design specification 3 becomes on the nominal closed-loop model $1.699e-03$, which is very high. Here again the weighting function is thus crucial to preserve closed-loop performance.

## IV. Conclusions

The primary aim of this paper was to illustrate the efficiency of the Convex Control Design tools on a challenging high-order flexible aircraft example, for checking the feasibility of a complex set of design specifications, with a feedback and feedforward part, and more generally for exploring the limits of achievable performance. As for a real-time implementation of the feedback controller, its order is too high, and it would be necessary to schedule it as a function of the flight conditions. To this aim the Convex Control Design tools can be combined with a modal reduction method that produces a possibly structured low-order controller preserving modal performance: this controller can then be easily scheduled as a function of the flight conditions.

## References

[1]Vroemen, B., and De Jager, B., "Multiobjective Control: An Overview," *Proceedings of the 36th IEEE Conference on Decision and Control*, Vol. 1, Inst. of Electrical and Electronic Engineers, New York, Dec. 1997, pp. 440–445.

[2]Campos-Delgado, D. U., and Zhou, K., "Mixed $L_1/H_2/H_\infty$ Control Design: Numerical Optimization Approaches," *International Journal of Control*, Vol. 40, No. 7, 2000, pp. 43–57.

[3]Alazard, D., "Robust $H_2$ Design for Lateral Flight Control of Highly Flexible Aircraft," *Journal of Guidance, Control, and Dynamics*, Vol. 25, No. 3, 2002, pp. 502–509.

[4]Lind, R., "Linear Parameter-Varying Modeling and Control of Structural Dynamics with Aerothermoelastic Effects," *Journal of Guidance, Control, and Dynamics*, Vol. 25, No. 4, 2002, pp.733–739.

[5]Haddad, W. M., and Chellaboina, V., "Mixed-Norm $H_2/L_1$ Controller Synthesis via Fixed-Order Dynamic Compemsation: A Riccati Equation Approach," *International Journal of Robust and Nonlinear Control*, Vol. 71, No. 1, 1998, pp. 35–59.

[6]Joos, H., "A methodology for Multi-Objective Design Assessment and Flight Control Synthesis Tuning," *Aerospace Science and Technology*, Vol. 3, No. 3, 1999, pp. 161–176.

[7]Boyd, S. P., and Barratt, C. H., *Linear Controller Design. Limits of Performance*, Prentice–Hall, New York, 1991.

[8]Pernebo, L., "An Algebraic Theory for the Design of Controller for Linear Multivariable Systems," *IEEE Transactions on Automatic Control*, Vol. 26, No. 1, 1981, pp. 171–194.

[9]Youla, D. C., Jabr, H. A., and Bongiorno, J. J., "Modern Wiener-Hopf Design of Optimal Controllers—Part II: The Multivariable Case," *IEEE Transactions on Automatic Control*, Vol. 21, No. 3, 1976, pp. 319–338.

[10]Alazard, D., and Apkarian, P., "Observer-Based Structures of Arbitrary Compensators," *International Journal of Robust and Nonlinear Control*, Vol. 9, No. 2, 1999, pp. 101–118.

[11]Khaisongkram, W., and Banierdpongchai, D., "MATLAB Based GUIs for Linear Controller Design via Convex Optimization," *Computer Applications in Engineering Education*, Vol. 11, No. 1, 2003, pp. 13–24.

[12]Hbaieb, S., Font, S., Bendotti, P., and Falinower, C. M., "Convex Optimal Control Design via Piecewise Linear Approximation," *Proceedings of the IFAC World Congress*, 2002.

[13]Lintereur, B. V., and McGovern, L. K., "Constrained $H_2$ Design via Convex Optimization Applied to Precision Pointing Attitude Control," *Proceedings of the 36th IEEE Conference on Decision and Control*, Vol. 2, Inst. of Electric and Electronic Engineers, New York, 1997, pp. 1389–1394.

[14]Ferreres, G., and Dardenne, I., "LP Synthesis of a Lateral Flight Control System for a Transport Aircraft," *Proceedings of the AIAA GNC Conference*, Vol. 1, 1997, pp. 155–164.

[15]Puyou, G., Ferreres, G., Chiappa, C., and Menard, P., "Multiobjective Method for Flight Control Law Design," *Proceedings of the AIAA GNC Conference*, 2004.

[16]McFarlane, D., and Glover, K., *Robust Controller Design Using Normalized Coprime Factor Plant Descriptions*, Lecture Notes in Control and Information Sciences, Springer-Verlag, New York, 1990.

[17]Hyde, R. A., and Glover, K., "The Application of Scheduled $H_\infty$ Controllers to a VSTOL Aircraft," *IEEE Transactions on Automatic Control*, Vol. 38, No. 7, 1993, pp. 1021–1039.

[18]Akcay, H., and Ninness, B., "Orthonormal Basis Functions for Continuous-Time Systems and Lp Convergence," *Mathematics of Control, Signals and Systems*, Vol. 12, No. 3, 1999, pp. 295–305.

[19]Kao, C. Y., Megretski, A., and Jonsson, U. T., "An Algorithm for Solving Optimization Problems Involving Special Frequency Dependent LMIs," *Proceedings of the 2000 American Control Conference*, Vol. 1, American Automatic Control Council, Danvers, MA, 2000, pp. 307–311.

[20]Packard, A., and Doyle, J., "The Complex Structured Singular Value," *Automatica*, Vol. 29, No. 1, 1993, pp. 71–109.

[21]Ferreres, G., *A Practical Approach to Robustness Analysis with Aeronautical Applications*, Springer-Verlag, New York, 1999.

[22]Ferreres, G., Magni, J. F., and Biannic, J. M., "Robustness Analysis of Flexible Structures: Practical Algorithms," *International Journal of Robust and Nonlinear Control*, Vol. 13, No. 8, 2003, pp. 715–734.

[23]Kubica, F., "Flight Control Law Conception for Flexible Aircraft," Ph.D. Dissertation, ENSAE, 1995 (in French), Toulouse, France, Dec. 1995.

[24]Kubica, F., and Livet, T., "Flight Control Law Synthesis for a Flexible Aircraft," *Proceedings of the AIAA GNC Conference*, 1994.